Theoretical approach on microscopic bases of stochastic functional self-organization: quantitative measures of the organizational degree of the environment

2001 J. Phys. A: Math. Gen. 34 10013

(http://iopscience.iop.org/0305-4470/34/47/308)

INSTITUTE OF PHYSICS PUBLISHING JOURNAL OF PHYSICS A: MATHEMATICAL AND GENERAL

J. Phys. A: Math. Gen. **34** (2001) 10013–10028 PII: S0305-4470(01)21389-4

Theoretical approach on microscopic bases of stochastic functional self-organization: quantitative measures of the organizational degree of the environment

Sorinel Adrian Oprisan

Department of Psychology, University of New Orleans, New Orleans, LA 70148, USA

E-mail: soprisan@uno.edu

Received 18 January 2001, in final form 4 September 2001
Published 16 November 2001
Online at stacks.iop.org/JPhysA/34/10013

Abstract

There has been increased theoretical and experimental research interest in autonomous mobile robots exhibiting cooperative behaviour. This paper provides consistent quantitative measures of organizational degree of a two-dimensional environment. We proved, by the way of numerical simulations, that the theoretically derived values of the feature are reliable measures of aggregation degree. The slope of the feature's dependence on memory radius leads to an optimization criterion for stochastic functional self-organization. We also described the intellectual heritages that have guided our research, as well as possible future developments.

PACS numbers: 05.65.+b, 05.45.−a, 64.60.−I, 87.10.+e

1. Introduction

The coherent behaviour displayed for the transport task observed in social insects can be attributed to the common goal shared by the individuals along with an identical set of interaction rules. Seeley noted this effect while considering the collective decision making in honeybees [39]. By way of the social insects, nature is showing us how to build decentralized and distributed systems that are autonomous and capable of accomplishing tasks through the interaction of many simple and highly redundant agents. From their local perception to the mass effect that results in a global action these biological systems serve to elucidate the mechanisms thought to be at the heart of self-organizing behaviour, sometimes called stigmergic self-organization or swarm intelligence.

Stigmergy, as proposed by Grasse [21], is a model used to explain the regulation of building behaviour in termites. Stigmergy theory holds that transitions between sequences

of construction steps are regulated by the effect of previous steps. In more general terms, the theory has been used to explain and describe the process by which task activity can be regulated using only local perception and indirect communication through the environment as applied to algorithms for coordinating distributed building behaviour [40] and foraging tasks by multi-robot systems [4]. Deneubourg [11] showed that chemical cues could organize part of the building activities of termites through a self-organizing stigmergic process. In this case, the stimuli encountered by the termites (concentrations of construction pheromones) differ quantitatively. There seem to be other cases where the stimulating patterns of matter perceived by the insects, such as wasps, undergo qualitative changes [14, 25, 40].

The collective behaviour of ants, bees, and other eusocial insects [15, 28] provide striking existence proofs that systems composed of simple agents can accomplish sophisticated tasks in the real world. It is widely believed that the cognitive capabilities of these insects are very limited, and the complex behaviour is emergent out of interaction between the agents. Therefore, the purpose of modelling multiagent systems is twofold. It leads to a deeper understanding of social insects behaviour and provides a decentralized, efficient, approaches on robots task allocation [38, 41]. There is no consensus about the meaning of cooperative behaviour in robotics. There are definitions that take into account the *goal* [5], the *communication strategy* [27], the *optimization of a global characteristic* [37], etc. Cooperative robotics already developed few successful hardware/software models such as CEBOTS (CEllular roBOTics System) [17–19], ACTRESS (ACTor-based Robot and Equipments Synthesis System) [2, 3], SWARM [24], GOFER [9, 26], ALLIANCE/L-ALLIANCE [34, 35], etc. The motivation of our studies is twofold. First, there is a noticeable gap in the literature of cooperative robots regarding formal metrics for cooperation and system performance. While the notion of cooperation is difficult to formalize, such metrics will be very useful in characterizing the nature of agent interactions. Second, experimental studies might become more rigorous and thorough, for example, via standard benchmark problems and algorithms. It is necessary for claims about 'robustness' and 'near-optimality' to be appropriately quantified, and for dependences on various control parameters to be better understood [10].

The present study emphasizes that the mechanism of functional self-organization is the indirect communication between the autonomous agents through the environmental changes they operate. This stigmergic self-organization can be optimized in terms of required time steps to achieve a *goal*. In this study, the goal is to sort and make piles of different object-types. In order to compare models and/or sorting strategies we need a measure of 'goodness'. Among many possible choices we focus our interest in texture analyses. We found that three so-called *features*, used in the field of image processing, are suitable to provide quantitative measures of 'goodness' [6, 22, 23][1].

2. Functional self-organization concept

The environment is modelled as a periodic two-dimensional lattice. Each lattice site has one of a finite number of distinct states. Usually, the number of states is small but, in principle, any finite cellular automata (CA) model over a finite alphabet can be defined. The state of a cell (site) changes according to specific local rules. There are two distinct classes of automata: synchronous, which allows simultaneous update of the states for all cells at a time and asynchronous, which allows gradual update of states. The updating order can be deterministic or random in the case of asynchronous update model. The space and time discrete model above

[1] A proof of the theorem in the unpublished reference [22] is given in [6]

decribed is called cellular automata [29, 36]. The dynamics of CAs are essentially determined by the considered neighbourhood. There is an increasing interest in CA models of physical phenomena due to the simplicity of computational tasks and the great flexibility of models. A burgeoning branch of dynamical systems theory studies the emergence of well-characterized collective phenomena in systems consisting of a large number of individuals connected by non-linear couplings [16, 32].

2.1. Fix length and equally weighted memory registers

Deneubourg *et al* [11–13] introduced a theoretical model in order to explain the organizing capability of living things based on experimental observations of the collective behaviour in ants. The model mimics the ants' behaviour by most rudimentary perceptual, motor and strategic mechanisms. The main features of the Deneubourg *et al* [11–13] model are summarized in the following requirements: (1) every ant (or *robot-like-ant* (RLA)) has the capability to recognize the distributed *objects* and record, in its finite length *memory register*, the most recent encountered object-type; (2) RLAs have object-manipulation capacity, the capacity to pick up, transport and put down objects; (3) RLAs execute a Brownian motion. The memory is a shift register of fix length n, which records the presence ('1') or absence ('0') of a specified object-type at the RLS's previous location. The most recent object-type encountered is memorized on the most significant bit place by shifting the old record with one place and remove the oldest entry in the register (the least significant bit). At every time step, every RLA generate a random number p obtained from a uniform distribution, and manipulates the objects (pick-up and put them down) as a function of p and a threshold (see [11–13] for mathematical details). The multirobotic network based on these rules has the capability to sort objects into piles by their specific property ('colour'). This sorting behaviour is emergent meaning that the RLAs are not explicitly programmed to sort the objects in order to form clusters.

2.2. The weighted memory model of functional self-organization

The above-cited model does not perform very well when the concentration of the objects is low (less than 1%). Moreover, the finite length of the memory and the equal weights given to all the recorded events determines wrong decisions and slows down the computation.

Our new model of stochastic functional self-organization (SFSO) is based on the following assumptions [30, 31]: (1) The lattice sites are occupied by physical objects, denoted by *a, b, c,* ... A free site is occupied by a ϕ object-type; (2) At any moment an RLA carries an object. The transported object may be of ϕ-type (free robot). The robots move randomly through the lattice, only one robot being allowed at one site; (3) When a robot moves to a given site it must decide if there are conditions to put down the carrying object and to pick up the existing one. The swapping condition is

$$f_\alpha \geqslant f_\beta \tag{1}$$

where f_α is the weighted frequency of the carried α-type object, and f_β is the weighted frequency of the encountered, β-type object. According to our newly proposed algorithm [30, 31], if the carried object was met more frequently than the encountered one then the RLA decides to swap the two objects. For example, let us refer to the following memorized string

$$\begin{array}{ll} & \Downarrow \quad \text{the most recent entry in the memory} \\ s_\tau: & b \quad b \quad b \quad b \quad b \quad a \quad a \quad a \quad a \quad a \end{array} \tag{2}$$

which indicates that the RLA has met five a-type objects and five b-type objects in the past. In order to simplify the numerical evaluations, any RLA associates a binary string to every object-type. Therefore, using the string (2) as an example, the binary string associated to a-type object is

$$s_a: \quad 0 \quad 0 \quad 0 \quad 0 \quad 0 \quad 1 \quad 1 \quad 1 \quad 1 \quad 1. \tag{3}$$

Generally specking, a binary string of length τ associated to an arbitrary α-type object has the form

$$s_{\alpha,\tau}: \quad u_{\alpha,1} \quad u_{\alpha,2} \cdots u_{\alpha,\tau} \tag{4}$$

where

$$u_{\alpha,i} = \begin{cases} 1 & \text{if } \alpha\text{-type object was encountered at the step } i \\ 0 & \text{otherwise.} \end{cases} \tag{5}$$

Based on (4) and (5), the following conservation rules take place: $\sum_{i=1}^{\tau} u_{\alpha,i} = n_\alpha$, for any $\alpha = \overline{1, T}$, where n_α is the total number of α-type objects encountered, and $\sum_{\alpha=1}^{T} u_{\alpha,i} = 1$, for any $i = \overline{1, \tau}$, where T is the total number of distinct object-types.

In order to make a decision, we proposed to characterize every object-type, at any instant τ, by a weighted frequency [30, 31]

$$f_\alpha(\tau) = \frac{\sum_{i=1}^{\tau} w(i) u_{\alpha,i}}{\sum_{i=1}^{\tau} w(i)} \tag{6}$$

where $w(i)$ is an appropriate *weighting function*. To surpass the shortcomings of other functional self-organization mechanism [11–13], we used for the first time [30, 31] a recursive defined memory that allows a whole history record. The proposed weighting function is [30, 31]

$$w(i) = \frac{1}{r^{i-1}}. \tag{7}$$

Using (7) and (6), one obtains

$$f_\alpha(K) = r^{K-1} \frac{r-1}{r^K - 1} \sum_{i=1}^{K} \frac{u_{\alpha,i}}{r^{i-1}}. \tag{8}$$

Based on (8), it can be seen that if $r \gg 1$ then the contribution of the τth step (for $\tau \gg 1$) to current swapping decision becomes insignificant [30, 31]. Therefore, only the most recent steps contribute to decision or, the system has a *short-type memory*. The limit case $r = 1$ corresponds to an infinite length of the memory and equally weighted events. The case when $r < 1$ exacerbates the contribution of the steps with $\tau \gg 1$ and diminishes the contribution of the most recent ones [1, 20]. Present study addresses only the case $r > 1$. For example, applying the weighting function (7) to string (3) one obtains $\frac{f_a(\tau)}{f_b(\tau)} = \frac{1}{r^5} < 1$, which shows that the RLA do not allow swapping if an a-type object is transported and it encountered a b-type object.

3. Overview of the analytical and numerical results on functional self-organization based on weighted memory algorithm

The particular form (7) of the weighting function was chosen in order to simplify the computational task. Let us observe that every time we compare two weighted frequencies the

denominator of (7) is the same and it can be omitted. Therefore, to make a decision, it is sufficient to compute at any instant the sum [31]

$$S_\alpha^n = \sum_{i=1}^{\tau} (u_{\alpha,i})_n w(i) \tag{9}$$

where $(u_{\alpha,i})_n$ is the binary digit corresponding to the ith place in the α string at the nth iteration step. Next step requires a new evaluation of the sum

$$S_\alpha^{n+1} = \sum_{i=1}^{\tau+1} (u_{\alpha,i})_{n+1} w(i) \tag{10}$$

where the following shifting rule takes place:

$$\begin{aligned} (u_{\alpha,i})^{n+1} &= (u_{\alpha,i-1})^n \quad \text{for } i \geqslant 2 \\ (u_{\alpha,1})^{n+1} &= \begin{cases} 1 & \text{if the } \textit{object} \text{ left in the current site is of } \alpha\text{-type} \\ 0 & \text{otherwise.} \end{cases} \end{aligned} \tag{11}$$

Using (11), (10) and (9) it results that

$$S_\alpha^{n+1} = \frac{1}{r} S_\alpha^n + (u_{\alpha,1})^{n+1} w(1). \tag{12}$$

There is no loss of information using the proposed form (7) of the weighted memory function because the recurrent sum (12) is a closed relationship. Moreover, to compute and compare the two sums, S_α^{n+1} and S_α^n, at a give instant, we need only two memory cells for every object-type: one for the old sum S_α^n and another for the new entry, $u_{\alpha,1}^{n+1}$ [30, 31].

3.1. Machine error limit of first-order recurrent memory

Despite its simplicity, the first-order recurrent schema (12) does not allow a truly infinitely long path record. This limitation is given by the internal finite digit representation of any real number [30, 31]. Indeed, let us consider two different strings

$$\begin{aligned} &s_\alpha(\tau)\text{: } u_\alpha(1)u_\alpha(2)\cdots u_\alpha(\tau) \\ &s_\beta(\tau)\text{: } u_\beta(1)u_\beta(2)\cdots u_\beta(\tau) \end{aligned} \tag{13}$$

with identical digits on their most significant τ_0 places ($u_\alpha(\tau) = u_\beta(\tau)$, for $i = 1, \ldots, \tau_0$). The maximum value of the difference between the two corresponding weighted frequencies is

$$\begin{aligned} \max |f_\alpha(N) - f_\beta(N)| &= \max \left| r^{N-1} \frac{r-1}{r^N - 1} \sum_{i=1}^{N} (u_\alpha(i) - u_\beta(i))^n w(i) \right| \\ &= r^{N-1} \frac{r-1}{r^N - 1} \sum_{i=\tau_0+1}^{N} \frac{1}{r^{i-1}} \leqslant \frac{1}{r^{\tau_0}}. \end{aligned} \tag{14}$$

The two different memorized strings will be considered numerically identical if $\max |f_\alpha(N) - f_\beta(N)| \leqslant \epsilon$, where ϵ is the computer internal error due to the finite digits internal representation of any real number. Based on the above formula, we may conclude that, in fact, the first order recurrent schema works with a finite effective memory whose length is given by

$$\tau_0 = -\frac{\ln \epsilon}{\ln r}. \tag{15}$$

The dependence of *the effective memory length* on the *memory radius* (r) and the numerical error is shown in figure 1.

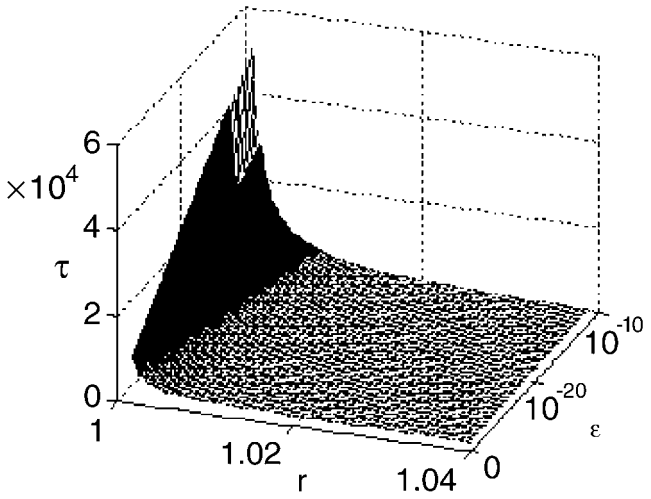

Figure 1. The dependence of the effective memory length on memory radius r and internal numerical error ϵ. As r approaches unity (infinite memory length with equally weighted records) the effective memory abruptly increases but remains finite due to finite numerical error of any real number internal representation.

3.2. The influence of multiple-valued mapping of Markov chains on local decisions

The main reason to change the Deneubourg's algorithm [11–13] was that, in order to decide about swapping, the RLAs have to consider the whole history and not an arbitrarily truncated Markov chain. Instead of a *short-term memory of m steps* [11–13], which records what was met in each of the last m steps, we consider that every RLA has a recursive cumulative memory for every object-type. Every microscopic-based model needs an appropriate global (cumulative) quantity over the whole (finite or infinite) record. In Deneubourg's model, the global measure was simply the mean of the binary record. We considered here, as a more realistic solution, a weighted mean value. However, the global measure over the memory record is not a univocal application from the (finite or infinite dimensional) vector space of the records to real numbers. It is possible to obtain the same global measure for different records and, therefore, to make bad decisions. To evaluate the probability of a bad decision, let $\mathcal{R}^N$ be the real N-dimensional vector space and $\mathcal{B} = (e_1, \ldots, e_N)$ its canonical basis. A random Markov chain of length N is a vector of the $\mathcal{R}^N$ space and can be written using $\mathcal{B}$ basis. Every algorithm for the functional self-organization maps the vector space $\mathcal{R}^N$ into the $\mathcal{R}$. A bad swapping decision appears when two different strings from $\mathcal{R}^N$ are mapped into the same point in $\mathcal{R}$. Let us consider two different strings s_1 and $s_2 \in \mathcal{R}^N$. Using (6), we found the number of different strings for a given memory radius r such that $f_\alpha^{s_1} - f_\beta^{s_2} = 0$, where α and β refer to the object-types under the swapping decision. The above condition reduces to $P\left(\frac{1}{r}\right) = a_0 + a_1\frac{1}{r} + \cdots + a_N\frac{1}{r^{N-1}} = 0$, where a_k are the polynomial coefficients of the associated N-step Markov chain. In the binary case, the only possible values for these coefficients are ± 1. Based on the Fermat theorem, the above restriction reduces to $P(0) \cdot P(1) < 0$ or, in a more useful form, $a_0(a_0 + a_1 + \cdots + a_N) < 0$. For an even number of coefficients $N = 2k$ the number of different coefficients determine the number of different strings which can be confounded, namely $S = \sum_{j=0}^{k-1} C_{2k}^{2k-j}$. For an odd number of coefficients, $N = 2k+1$, this number becomes $S = \sum_{j=-1}^{k-2} C_{2k+1}^{2k-j}$. Based on above estimations, we found that the probability to make a bad decision is $p < 10^{-5}$ for $\tau = N > 10$.

3.3. The convergence of the algorithm

At the theoretical level, the main question regards the convergence of the functional self-organization algorithm. Convergence means that the long time dynamics displays the desired goal, namely realizes objects' sorting in order to form some desired patterns (clusters, stripes, chess-like board, etc.) [31].

First, we prove the necessary convergence condition in order to start the aggregation of identical object-type clusters. To this purpose, let us consider, without any loss of generality, that initially an RLA had met an a-type object and picks it up. Then, let us suppose that the RLA moved through a field entirely occupied by the b-type objects and, after τ steps, it met again an a-type object. The less favourable memorized string for the a-type object is $u_a(\tau)$:$\overbrace{100\cdots0}^{\tau}$, where the last entry indicates that the RLA had met only one a-type object. The corresponding string for the b-type objects is $u_b(\tau)$:$\overbrace{011\cdots1}^{\tau}$. The necessary condition to put down the carried a-type object in the neighbourhood of the last a-type object encountered is $f_a(\tau) \geqslant f_b(\tau)$, which, using (6), can be written $r^{\tau+1} - 2r^{\tau} + 1 \geqslant 0$. This relationship is fulfilled if and only if $r \in [1, r_{0,\tau}) \cup (2, \infty)$, where $r_{0,\tau}$ is the root of the equation $r^{\tau+1} - 2r^{\tau} + 1 = 0$, in $(1, 2)$ interval. Therefore, even in the less favourable case, it is possible to choose an appropriate memory radius value r in order to form a cluster with two identical objects. Once this cluster has been formed, it starts to grow. On the other hand, the algorithm converges for any concentration of the objects and this is one of the most important achievements of the present model.

Next question is: how long will it take to reach the less probable configuration, or, equivalently, which is the probability to occur the associated Markov chain? To estimate the probability we used a mean field approach. We assumed that the probability to find an object in a given lattice site is not determined by the other objects' positions. Therefore, the probability to find an object, say of a-type, can be approximated by $p_a = c_a \frac{v}{V} = c_a \frac{4}{V}$, where $c_a = \frac{N_a}{N}$ is the concentration of the a-type objects, v is the 'volume' (area) of the neighbourhood and V is the lattice 'volume' (area). Let $p_{a,i}$ be the probability to find $i \in \{0, 1, 2, 3, 4\}$ a-type objects in the neighbourhood of an arbitrary site. Under above assumptions, an approximation of this probability is given by the binomial distribution $p_{a,i} = \binom{i}{N_a} p_a^i (1 - p_a)^{N_a - i}$. Under these conditions, the mean number of the a-type objects in the neighbourhood of an arbitrary lattice site is given by

$$\bar{\xi}_a = \frac{\sum_{i=0}^{4} i p_{a,i}}{\sum_{i=0}^{4} p_{a,i}} = \frac{\sum_{i=0}^{4} i \binom{i}{N_a} p_a^i (1 - p_a)^{N_a - i}}{\sum_{i=0}^{4} \binom{i}{N_a} p_a^i (1 - p_a)^{N_a - i}}. \tag{16}$$

The above relation allows to write the mean probability to find an a-type object in the neighbourhood of an arbitrary lattice site in the form $\bar{p}_a = \frac{1}{4}\bar{\xi}_a$, and for the b-type objects $\bar{p}_b = \frac{1}{4}\bar{\xi}_b = \frac{1}{4}(4 - \bar{\xi}_b) = 1 - \bar{p}_b$. In order to obtain the probability to realize the less favourable path we make the following assumptions: (1) jumps are independent events (random walk), (2) the first object encountered by RLA was of a-type with the probability $\frac{N_a}{N}$ and picked it up, (3) the RLA moves $\tau - 2$ steps through the lattice finding only b-type objects, (4) finally, the RLA meets another a-type object. Using all of the above conditions, one obtains

$$p_{\min} = \frac{N_a}{N}(1 - \bar{p}_a)^{\tau-2} \bar{p}_a \tag{17}$$

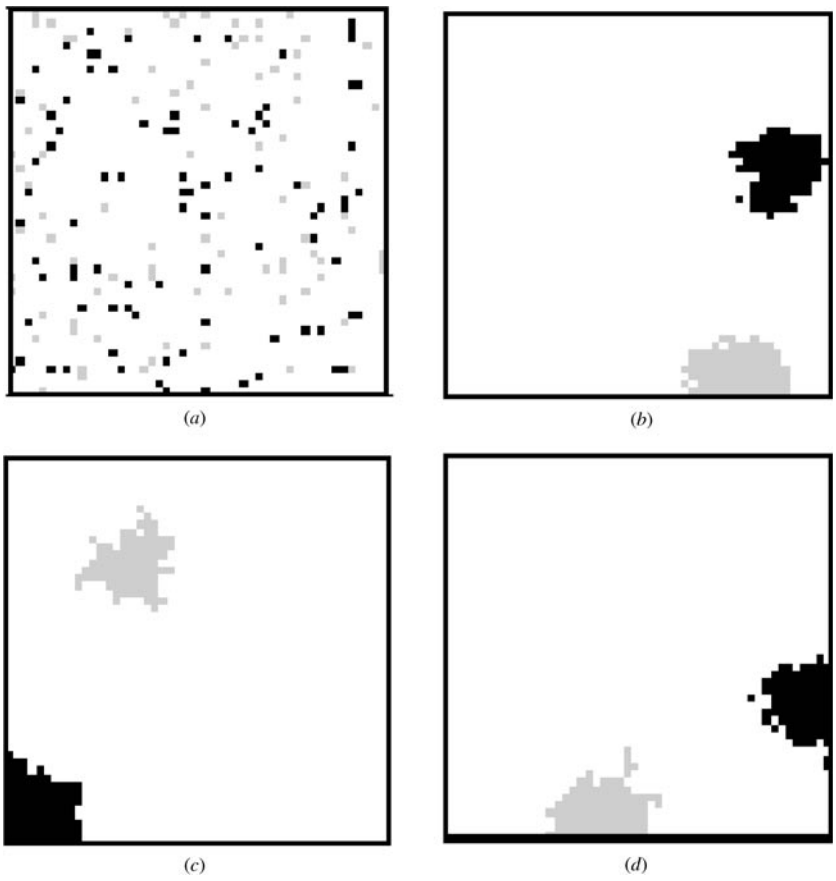

Figure 2. Initial random configuration (a) in a 50×50 two-dimensional periodic lattice containing $N_a = N_b = 100$ objects to be sorted by 30 RLAs. Clusters appear for $r = 1.1$ after 2.5×10^5 steps (b), $r = 1.3$ after 6.5×10^5 steps (c) and $r = 1.5$ after 10^6 steps (d). This fact indicates that the memory radius is an important control parameter in order to optimize numerical computation.

where the first factor is taken because the RLA met an a-type object at the first step with the probability $\frac{N_a}{N}$ and that object is then carried $\tau - 1$ steps until another a-type object is found. It follows that the maximum number of steps which ensures convergence is

$$\mathcal{N}_{\max} = \frac{1}{p_{\min}} = \frac{N}{N_a} \frac{1}{\bar{p}_a (1 - \bar{p}_a)^{\tau - 2}}. \tag{18}$$

To minimize the computational time, the memory radius r must change during simulations.

3.4. Numerical results on cluster aggregation

We performed numerical simulations using the memory function based on the weighted relative frequencies (8). The most significant control parameter in our model is the memory radius r. All the present results were obtained using a constant value for the memory radius during computations. Numerical simulations confirmed our theoretical result regarding the convergence of the algorithm. Moreover, using different values for the memory radius r we found that the average number of Monte Carlo timesteps required to achieve the final sorting stage increases if r increases (see figure 2). Intuitively this result seems to be correct because

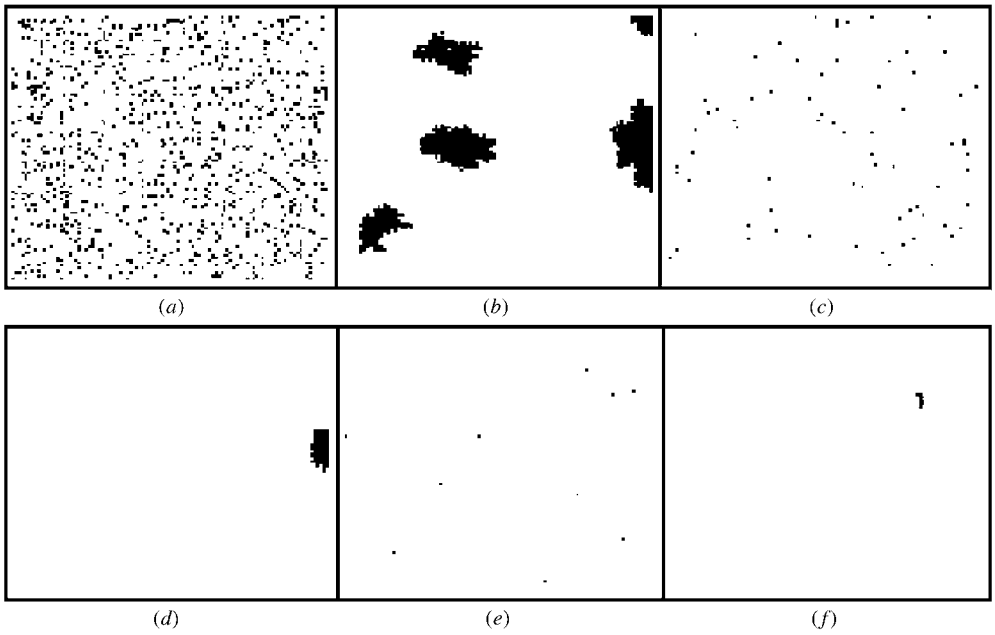

Figure 3. The stochastic functional self-organization mechanism successfully builds clusters even with a very low concentration of the distributed objects. The environment is a 50×50 periodic two-dimensional lattice with 30 RLAs. A 10% concentration of a-type objects is randomly distributed (a). If the memory radius is $r = 1.1$, then the final aggregation stage is reached after 2.5×10^5 Monte Carlo timesteps (b). When the initial random concentration is 1% (panel c) and the memory radius $r = 1.3$ the required conventional time is 6.5×10^5 (see panel d). Finally, an initially random distribution of the objects with 0.1% concentration and $r = 1.5$ requires 10^6 conventional timesteps to reach the final aggregation stage. These results indicate that the concentration of the objects is another important parameter when we deal with optimization problem.

a high value of the memory radius means a short-range temporal correlation between the recorded bits. This kind of memory is definitely helpful at the incipient stage of aggregation and allows a fast separation of small clusters. Unfortunately, keeping a high value for the memory radius slows down the aggregation of bigger clusters because the short-range memory correlations cannot cover the increasing correlation pattern.

The convergence of the stochastic functional self-organization algorithm based on weighted memory function was also tested for different values of the object concentrations. We found that the algorithm converges even for as low concentrations as .1% (see figure 3).

Based both on theoretical results we proved and numerical simulations, we can say that the capability of the above described multirobotic network to perform the sorting process manifests for any $r > 1$ and the convergence speed (the minimum number of Monte Carlo conventional steps required in order to reach the final steady state sorting configuration) depends sensibly on r.

4. Local and global measures of the organization degree

The computation with the stochastic functional self-organization based on weighted memory algorithm requires a well-defined criterion in order to stop the simulations. On the other hand, in order to classify the pattern and/or to compare the aggregation velocity for different

memory radius values r and/or to extract parameters of the phenomenological model (diffusion coefficient, mean swapping frequency, mean elapsed time between swapping, etc) we need quantitative measures of the aggregation process. One possibility is to use a locally orientated criteria. The ability of the RLAs to reduce global environment entropy can be traced to their primitive capacity to perceive complexity locally and behave accordingly. Complexity and entropy are closely related concepts. While entropy can be reliably measured on a global scale, it is difficult to find an adequate measurement of entropy on a local scale [41]. The local orientated measure of complexity uses a nine-cell neighbourhood in the rectangular lattice. The complexity of the neighbourhood is taken as the number of faces that separate cells of different object types. The RLA uses the locally measured complexity to direct their physical motion and their object manipulation as well as to decide, statistically, to stop the aggregation process. The second possible approach refers to some globally defined functions (measures) that are not available to every RLA computation. The second method is more adequate to extract some quantitative measures about the aggregation stage.

The present study addresses the usefulness of global measures called *features* associated with textures [22]. The texture analysis using features considers that texture-context information is contained in the overall spatial relationship between the gray tones. Let $p(i, j)$ be the normalized matrix of relative frequencies with which two neighbouring resolution cells separated by distance d occur on the image, one with gray tone i and the other with gray tone j. The matrix of gray-tone spatial-dependence frequencies depends on angular relationship between the neighbouring cells. In the following, we will refer only to horizontal gray-tone spatial-dependence matrix but it is easy to obtain, in the same way, any other matrix. To characterize simple textures only three global features are needed:

The angular second-moment feature is a measure of homogeneity of the image. In a homogeneous image this feature has a great value and decreases if the texture becomes less homogeneous (texture with different clusters)

$$f_1 = \sum_{i=1}^{N_g} \sum_{j=1}^{N_g} p(i, j)^2 \tag{19}$$

where N_g is the number of gray tone in the texture.

Contrast is the measure of amount of local variations present in the image

$$f_2 = \sum_{n=0}^{N_g-1} n^2 \left(\sum_{|i-j|=n} p(i, j) \right). \tag{20}$$

Correlation is a measure of gray-tone linear dependence in the image

$$f_3 = \frac{1}{\sigma_x \sigma_y} \left(\sum_{i=1}^{N_g} \sum_{j=1}^{N_g} ijp(i, j) - \mu_x \mu_y \right) \tag{21}$$

where μ_x, μ_y are the mean and σ_x, σ_y are the standard deviations of the vectors $p_x(i) = \sum_{j=1}^{N_g} p(i, j)$ and $p_y(j) = \sum_{i=1}^{N_g} p(i, j)$, respectively. In a noisy sample there is no correlation between the gray-tones and therefore the correlation features has a low value.

4.1. Analytical evaluation of the relevant features for a completely sorted two-dimensional picture

In the following, the environment is a periodic two-dimensional lattice and only three-object type, denoted by letters a, b and ϕ (empty sites), respectively, were considered. Let $N_{\text{int}}(i)$

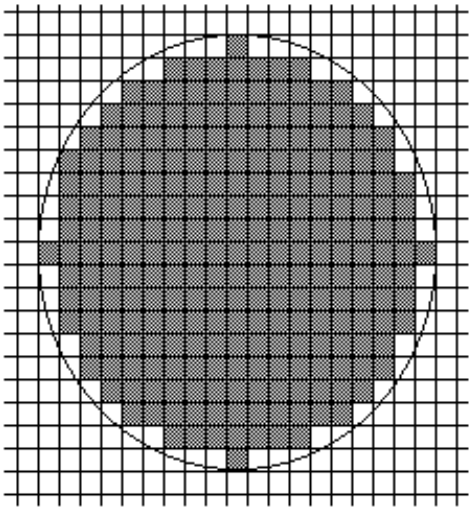

Figure 4. Symmetric cluster of *a*-type object (grey) in a two-dimensional rectangular lattice. This structure was observed, as final steady state, in numerical simulations. Therefore, it was considered the most probable configuration at the end of the aggregation process. Based on this configuration, the values for the features were derived.

be the number of the lattice sites inside the i-type objects' clusters and $N_{\text{ext}}(i)$ the number of the lattice sites on the border of the same cluster (see figure 4). Taking into account only the nearest neighbour interaction, a rough estimation of the spatial-dependence matrix entries is

$$p(i,i) = \frac{1}{N}\left(2N_{\text{int}}(i) + (N_{\text{ext}}(i))_x\right) \tag{22}$$

where N is a normalization factor and $(N_{\text{ext}}(i))_x$ is the number of the lattice sites on the border of the i-type clusters in the horizontal direction. For the symmetric clusters, this number can be approximated by $(N_{\text{ext}}(i))_x \approx (N_{\text{ext}}(i))_y = \frac{1}{2}N_{\text{ext}}(i)$. To simplify further evaluations, we adopt a numerical equivalence for the object-types (a, b, ϕ) and the set (1, 2, 3) and we assume that the greatest occupation number belongs to ϕ object-type (empty site). In the complete sorting stage, the a-type objects' cluster and the b-type objects' cluster have no common lattice site. Therefore, taking into account the symmetry of the spatial-dependence matrix, it follows $p(1,2) = p(2,1) = 0$, $p(1,3) = p(3,1) = \frac{1}{N}(N_{\text{ext}}(1))_x$ and $p(2,3) = p(3,2) = \frac{1}{N}(N_{\text{ext}}(2))_x$, respectively. Using (22) and above symmetry-related relationships, the corresponding matrix of symmetric pattern (see figure 4) is

$$(P) = \frac{1}{N}\begin{pmatrix} 2N(1) - \frac{3}{2}N_{\text{ext}}(1) & 0 & \frac{1}{2}N_{\text{ext}}(1) \\ 0 & 2N(2) - \frac{3}{2}N_{\text{ext}}(2) & \frac{1}{2}N_{\text{ext}}(2) \\ \frac{1}{2}N_{\text{ext}}(1) & \frac{1}{2}N_{\text{ext}}(2) & 2N(3) - \frac{3}{2}N_{\text{ext}}(3) \end{pmatrix} \tag{23}$$

where $N = 2(N(1) + N(2) + N(3)) - \frac{1}{2}(N_{\text{ext}}(1) + N_{\text{ext}}(2)) - \frac{3}{2}N_{\text{ext}}(3)$. The boundary length conservation writes $N_{\text{ext}}(3) = N_{\text{ext}}(1) + N_{\text{ext}}(2)$ and the conservation of the objects' number gives $N(1) + N(2) + N(3) = N_x N_y$, where N_x (N_y) is the total number of horizontal (vertical) lattice sites. Using above conservation rules, it results that

$$N = 2\left[N_x N_y - (N_{\text{ext}}(1) + N_{\text{ext}}(2))\right]. \tag{24}$$

Let us denote by $c_i = \frac{N(i)}{N_x N_y}$ the concentration of the i-type object. If the cluster dimension $N(i)$ is big enough then a rough estimation of the number of the lattice sites on its border is $N_{\text{ext}}(i) \approx \alpha\sqrt{N(i)}$, where $\alpha \in (0,1)$ is a constant. Substituting the above relationship into (24) it can be obtained

$$N \approx 2N_x N_y\left[1 - \alpha\frac{\sqrt{N(1)} + \sqrt{N(2)}}{N_x N_y}\right] = 2N_x N_y\left[1 - \alpha\left(\sqrt{\frac{c_1}{N_x N_y}} + \sqrt{\frac{c_2}{N_x N_y}}\right)\right]. \tag{25}$$

Substituting (25) into (23) and using the notation $y = \frac{\alpha}{\sqrt{N_x N_y}}$ it results that

$$(P) = \frac{1}{1 - y\left(\sqrt{c_1} + \sqrt{c_2}\right)} \begin{pmatrix} c_1 - \frac{3}{4} y\sqrt{c_1} & 0 & \frac{y}{2}\sqrt{c_1} \\ 0 & c_2 - \frac{3}{4} y\sqrt{c_2} & \frac{y}{2}\sqrt{c_2} \\ \frac{y}{2}\sqrt{c_1} & \frac{y}{2}\sqrt{c_2} & c_3 - \frac{3}{4} y\sqrt{c_3} \end{pmatrix} \tag{26}$$

where c_i are related by $c_1 + c_2 + c_3 = 1$. According to the definition (19), and using the matrix (26), one obtains

$$\begin{aligned} f_1 = \sum_{i=1}^{3}\sum_{j=1}^{3} p(i,j)^2 &= \frac{1}{\left[1 - y\left(\sqrt{c_1} + \sqrt{c_2}\right)\right]^2} \\ &\times \left[c_1^2 + c_2^2 + c_3^2 - \frac{3}{2} y\left(c_1^{\frac{3}{2}} + c_2^{\frac{3}{2}} + c_3^{\frac{3}{2}}\right) + y^2\left(\frac{17}{16}c_1 + \frac{17}{16}c_2 + \frac{9}{16}c_3\right)\right] \end{aligned} \tag{27}$$

In the same way, using (20) it results that

$$f_2 = \sum_{n=0}^{2} n^2 \left(\sum_{i,j;|i-j|=0}^{3} p(i,j)\right) = \frac{y\left(2\sqrt{c_1} + \sqrt{c_2}\right)}{1 - y\left(\sqrt{c_1} + \sqrt{c_2}\right)}. \tag{28}$$

The corresponding reduced matrices are:

$$\begin{aligned} p_x &= \frac{1}{1 - y\left(\sqrt{c_1} + \sqrt{c_2}\right)} \\ &\times \left(c_1 - \tfrac{y}{2}\sqrt{c_1} \quad c_2 - \tfrac{y}{2}\sqrt{c_2} \quad c_3 - \tfrac{3y}{2}\sqrt{c_3} + y\left(\sqrt{c_1} + \sqrt{c_2}\right)\right) \\ p_y^{\mathrm{T}} &= \frac{1}{1 - y\left(\sqrt{c_1} + \sqrt{c_2}\right)} \\ &\times \left(c_1 - \tfrac{y}{2}\sqrt{c_1} \quad c_2 - \tfrac{y}{2}\sqrt{c_2} \quad c_3 - \tfrac{3y}{2}\sqrt{c_3} + y\left(\sqrt{c_1} + \sqrt{c_2}\right)\right) \end{aligned} \tag{29}$$

where the superscript T means transposition. It follows from (29) that the mean value and standard deviation are given by

$$\begin{aligned} \mu_x &= \sum_{i=1}^{3} i p_x(i) = \frac{1}{1 - y\left(\sqrt{c_1} + \sqrt{c_2}\right)}\left[c_1 + 2c_2 + 3c_3 + \frac{y}{4}\left(5\sqrt{c_1} + 6\sqrt{c_2} - 9\sqrt{c_3}\right)\right] \\ \sigma_x^2 &= \sum_{i=1}^{3}(i - \mu_x) p_x(i) = \sum_{i=1}^{3} i^3 p_x(i) - (\mu_x)^2 \\ &= \frac{1}{\left[1 - y\left(\sqrt{c_1} + \sqrt{c_2}\right)\right]^2}\Big[\left(1 - y\left(\sqrt{c_1} + \sqrt{c_2}\right)\right)\left[c_1 + 2c_2 + 9c_3\right. \\ &\quad \left. + \frac{y}{4}\left(17\sqrt{c_1} + 14\sqrt{c_2} - 27\sqrt{c_3}\right)\right] - \left[c_1 - 2c_2 + 3c_3\right. \\ &\quad \left. + \frac{y}{4}\left(5\sqrt{c_1} + 4\sqrt{c_2} - 9\sqrt{c_3}\right)\right]^2\Big]. \end{aligned} \tag{30}$$

A major, realistic, simplification of (30) can be obtained by considering $y \ll 1$ (low object concentration) and $c_1 = c_2 = c$ (equal concentration of objects to be sorted). Finally, the three principal features mentioned above can be written

$$f_1 \approx 1 - 4c + 6c^2 + y\left[4\sqrt{c}\left(3c^2 - 2c + 1\right) - \frac{3}{2}\left(c^{\frac{3}{2}} + (1 - c)^{\frac{3}{2}}\right)\right]$$

$$f_2 \approx 5y\sqrt{c}\left(1+2y\sqrt{c}\right) \tag{31}$$
$$f_3 = \frac{c(5-9c)+y/4\left[21\sqrt{c}-27\sqrt{1-2c}-6(1-c)\left(8(4-3c)\sqrt{c}-9\sqrt{1-2c}\right)\right]}{c(5-9c)+y/4\left[-95\sqrt{c}+27(1-2c)\sqrt{1-2c}+238c\sqrt{c}-144c^2\sqrt{c}\right]}.$$

If the lattice is big enough then $y \to 0$ and, therefore

$$f_1 \approx 1-4c+6c^2 \qquad f_2 \approx 0 \qquad f_3 = 1. \tag{32}$$

The values (31) and (32) of the features were obtained for the final stage of the aggregation process.

4.2. Analytical evaluation of the relevant features for a noisy two-dimensional picture

In order to complete the analytical description of aggregation process by global features we also evaluate the values for the initial (noisy) configuration. To this purpose, let us denote by *N(i, j)* the number of *i–j* nearest neighbour sites. According to our previous assumptions

$$\begin{aligned} &N(1,1)=N(2,2)=0 \qquad N(1,2)+N(1,3)=2N(1) \\ &N(2,1)+N(2,3)=2N(2) \qquad N(3,1)+N(3,2)+N(3,3)=2N(3). \end{aligned} \tag{33}$$

It is straightforward that the interface of ϕ-type objects with the other object-types gives $N(3,1)+N(3,2) \propto \sqrt{N(3)}$. Due to high symmetry of the noisy configuration, the following relations exist: $N(1,2)=N(2,1)=N_{12}$, $N(1,3)=N(3,1)=N_{13}$, $N(2,3)=N(3,2)=N_{23}$. Based on (33) and above relationships, the non-zero matrix elements are:

$$\begin{aligned} &N_{12}=N(1)+N(2)-\frac{\beta}{2}\sqrt{N(3)} \qquad N_{13}=N(1)-N(2)+\frac{\beta}{2}\sqrt{N(3)} \\ &N_{23}=-N(1)+N(2)+\frac{\beta}{2}\sqrt{N(3)} \qquad N_{33}=2N(3)-\beta\sqrt{N(3)} \end{aligned} \tag{34}$$

where $\beta \in (0,1)$ is a constant. Therefore, the normalized matrix of the noisy pattern is

$$(P)=\frac{1}{N}\begin{pmatrix} 0 & c_1+c_2-\frac{\beta}{2}\sqrt{\frac{c_3}{N_xN_y}} & c_1-c_2+\frac{\beta}{2}\sqrt{\frac{c_3}{N_xN_y}} \\ c_1+c_2-\frac{\beta}{2}\sqrt{\frac{c_3}{N_xN_y}} & 0 & -c_1+c_2+\frac{\beta}{2}\sqrt{\frac{c_3}{N_xN_y}} \\ c_1-c_2-\frac{\beta}{2}\sqrt{\frac{c_3}{N_xN_y}} & -c_1+c_2+\frac{\beta}{2}\sqrt{\frac{c_3}{N_xN_y}} & 2c_3-\beta\sqrt{\frac{c_3}{N_xN_y}} \end{pmatrix} \tag{35}$$

where $N=2N_x \times N_y$ is a normalization factor. If the lattice environment is large enough then (35) becomes

$$(P)=\frac{1}{N}\begin{pmatrix} 0 & c_1+c_2 & c_1-c_2 \\ c_1+c_2 & 0 & -c_1+c_2 \\ c_1-c_2 & -c_1+c_2 & 2c_3 \end{pmatrix}. \tag{36}$$

Using (36), one obtains the reduced matrix $p_x=(c_1 \quad c_2 \quad c_3)$, with the following mean and dispersion:

$$\begin{aligned} \mu_x &= \sum_{i=1}^{3} i p_x(i) = c_1+2c_2+3c_3 \\ \sigma_x^2 &= \sum_{i=1}^{3}(i-\mu_x)p_x(i) = \sum_{i=1}^{3} i^2 p_x(i)-(\mu_x)^2 \\ &= c_1+4c_2+9c_3+(c_1+2c_2+3c_3)^2. \end{aligned} \tag{37}$$

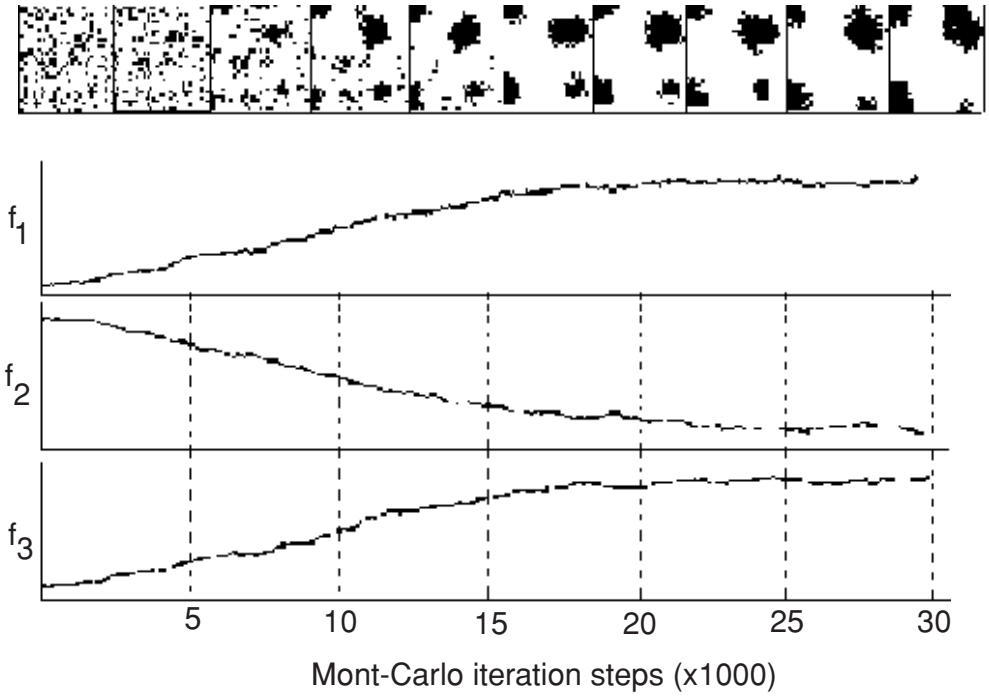

Figure 5. Qualitative picture of the environment (upper panel) and the corresponding quantitative measures (lower panel). Different snapshots of the two-dimensional lattice are uniformly sampled every 5000 Monte Carlo simulation steps (upper panel). The lower panel shows the time-dependence of the three features. Their initial and final values are in a very good agreement with the theoretically predicted results. The environment is a two-dimensional periodic lattice with 100 $\times$ 100 sites and 10% black objects' concentration. The task was performed by 40 RLAs with memory radius $r = 1.1$.

In the limit case $\beta\sqrt{\frac{c_3}{N_x N_y}} \to 0$, the principal features are

$$f_1 \approx 6c^2 - 4c + 1 \qquad f_2 \approx 2c \qquad f_3 \approx \frac{4 - 9c}{5 - 9c}. \tag{38}$$

4.3. Applications of the feature method to stochastic functional self-organization

Numerical simulations demonstrate that the above-defined features are sensitive to aggregation stage and offer a quantitative meaning of this fuzzy concept. In our numerical experiment a two-dimensional periodic lattice was considered. The memory radius r was fixed. Starting the aggregation process with an initially noisy configuration we recorded the picture of the lattice (upper panel of figure 5) and the corresponding values of the features (lower panel of figure 5). The purpose of the present computation is twofold. First, we checked that the initial and asymptotic values of the features are in a very good agreement with the theoretically predicted ones. Second, the numerical simulations proved that, for a fix value of the memory radius, there is a limited temporal domain that ensures a very fast change in the feature values followed by a long lasting temporal domain of clusters' shape adjustment. Based on numerical simulations performed with different memory radius values we may conclude that it is more advantageous, in order to reduce the computational effort, to start with a high value of the

memory radius. A high value of the memory radius means a very abrupt decrease of the features and a rapidly slowing down of the algorithm. If the simulation continues with such a high value of the memory radius the system needs a long computation to reach the steady state. Therefore, despite their very fast initial change in the feature values the system will slow down rapidly. On the other hand, a low memory radius will determine a slow change of the features but the end of the linear region is more close to the final steady state. Above observations are the basic ingredients for our optimization algorithm. Our optimization procedure searches for an appropriate dynamic change of the memory radius during the numerical simulation in order to balance the high speed of the feature change (for high values of memory radius) with the lowest quasi steady state of the linear region (for the low memory radius values). The optimization rule for stochastic functional self-organization exceeds the goal of the present paper and will be published elsewhere [33].

5. Conclusions

The present paper provides an overview of the main theoretical and numerical results concerning the stochastic functional self-organization mechanism (section 3) [1, 20, 30, 31]. The proposed distributed sorting algorithm is less efficient than a hierarchical organized system, but its great advantage is that it does not require any map of the environment, global representation or supervisor.

The paper proposes three quantitative *global* measures of organizational degree of a given two-dimensional environment (texture). The proposed quantitative measures are sensitive to spatial organization of the environment. We evaluated the initial values of the *features* for noisy configuration (random distribution of the objects) and totally sorted configuration with symmetric clusters. Our theoretically evaluated limits of the features are in very good agreement with the computational results. The dynamics of the proposed features (see figure 5) indicates that the speed of feature variation strongly depends on the memory radius r (control parameter). Our idea of optimization of the stochastic functional self-organization mechanism is as follows. First, an extensive numerical survey of the feature dynamics is necessary. The goal is to obtain the landscape of feature dependence on the number of iteration steps (time) and the memory radius (control parameter). Second, using the 3D landscape numerically derived, it is possible to find an optimum path through the landscape according to a given optimization criterion. In our case, minimization of the aggregation time could be an appropriate optimization criterion.

The present algorithm is based on first order recurrent memory. This particular fact imposes a very simple, not trivial, functional form of the weighting function. Our preliminary results indicate that a second order, non-monotonic, memory function is a more realistic model for human pattern analysis.

Acknowledgments

I express my gratitude to a number of people who become involved with these studies. My PhD thesis advisor, Professor Dr Margareta Ignat, whose suggestions led me throughout this research, has always been willing to answer my questions. Viorel Holban and Bogdan Moldoveanu, two exceptional friends, were so gracious in providing me some of the tools I needed for numerical simulations. I owe many thanks to my family who have been supportive of my academic venture.

References

[1] Amarie D, Oprisan S A and Ignat M 1999 *Phys. Lett.* A **254** 112
[2] Asama H, Matsumoto A and Ishida Y 1989 *IEEE/RSJ IROS* pp 283–290
[3] Asama H, Ishida Y, Ozaki K, Habib M K, Matsumoto A, Kaetsu H and Endo I 1992 *Proc. Japan USA Symposium on Flexible Automation* ed M Leu pp 647–654
[4] Beckers R, Holland O E and Deneubourg J-L 1994 *Proc. Fourth Int. Workshop on the Synthesis and Simulation of Living Systems Artificial Life IV* pp 181–189
[5] Barnes D and Gray J 1991 *Proc. Int. Conf. Control* pp 1135–1140
[6] Besag J E 1974 *J. R. Stat. Soc.* **36B** 192
[7] Boccara N, Goles E, Martinez S and Picco P (ed) 1993 *Cellular Automata and Cooperative Systems* (Dorderecht: Kluwer)
[8] Burks A (ed) 1970 *Essays on Cellular Automata* (Urbana-Champaign, IL: University of Illinois Press)
[9] Caloud P, Choi W, Latombe J-C, LePape C and Yin M 1990 *IEEE/RSJ IROS* pp 67–72
[10] Cao Y U, Fukunaga A S and Kahng A B 1997 *Auton. Robots* **4** 1
[11] Deneubourg J-L 1977 *Insectes Sociaux* **24** 117
[12] Deneubourg J-L, Pasteels J M and Verhaeghe J C 1983 *J. Theor. Biol.* **105** 259
[13] Deneubourg J-L and Goss S 1989 *Ethology Ecol. Evol.* **1** 295
[14] Downing H A and Jeanne R L 1988 *Anim. Behav.* **36** 1729
[15] Franks N R 1989 *Am. Sci.* **77** 139
[16] Frisch U, Hasslacher B and Pomeau Y 1986 *Phys. Rev. Lett.* **56** 1505
[17] Fukuda T and Nakagawa S 1987 *Proc. Int. Conf. Industrial Electronics, Control, and Instrumentation* pp 588–595
[18] Fukuda T, Kawauchi Y and Asama H 1990 *IEEE/RSJ IROS* pp 827–834
[19] Fukuda T and Iritani G 1995 *IEEE/RSJ IROS* pp 535–42
[20] Giuraniuc C V and Oprisan S A 1999 *Phys. Lett.* A **259** 334
[21] Grasse P *Insectes Sociaux* **6** 41
[22] Hammersly J M and Clifford P 1971 Markov field on finite graphs and lattices, unpublished
[23] Haralick R, Shanmugan K and Distein I 1973 *IEEE Trans. Syst. Man and Cybern.* **3** 610
[24] Jin K, Liang P and Beni G 1994 *IEEE ICRA* pp 1933–1038
[25] Karsai I and Theraulaz G 1995 *Sociobiology* **26** 83
[26] LePape C 1990 *IEEE ICRA* pp 488–493
[27] Mataric M 1994 Interaction and intelligent behavior *PhD Thesis,* MIT EESC Department
[28] McFarland D 1994 *Proc. 3rd Int. Conf. on Simulated Adaptive Behavior* (Cambridge, MA: MIT Press) pp 440–3
[29] Neumann von J 1996 *Theory of Self-Reproducing Automata* (Urbana-Champaign, IL: University of Illinois Press)
[30] Oprisan S A, Holban V and Moldoveanu B 1996 *Phys. Lett.* A **216** 303
[31] Oprisan S A 1998 *J. Phys. A: Math Gen.* **31** 8451
[32] Oprisan S A, Ardelean A and Frangopol P T 2000 *Bioinformatics* **60** 1
[33] Oprisan S A 2001 *Complex Syst.* at press
[34] Parker L E 1994 *IEEE/RSJ IROS* pp 776–783
[35] Parker L E 1994 Heterogeneous multi-robot cooperation *PhD Thesis,* EECS Department MIT, Cambridge, MA
[36] Perdang J M and Lejeune A (ed) 1993 *Cellular Automata* (Singapore: World Scientific)
[37] Premvuti S and Yuta S 1990 *IEEE/RSJ IROS* pp 59–63
[38] Rodin E Y and Amin S M 1989 *Proc. Intelligent Symp. Intelligent Control (Alexandria, VA)* pp 366–369
[39] Seeley T D, Camazine S and Sneyd J 1991 *Behav. Ecol. Sociobiol.* **28** 277
[40] Theraulaz G and Bonabeau E 1995 *Science* **269** 686
[41] Unsal C 1993 Self-organisation in large population of mobile robots *MS Thesis* Virginia Polytechnic Institute